

QUANTUM INTERFERENCE AND POLING IN OPTICAL GLASS WAVEGUIDES

1727

P. G. Kazansky

Optoelectronics Research Centre, University of Southampton,
Southampton SO17 1BJ, United Kingdom
E-mail: pgk@orc.soton.ac.uk

Optical glass fibres and waveguides dominate optical communications. The development of linear electrooptic modulators/switches and parametric frequency converters directly integrated into optical glass waveguide structures technologically is very attractive. However such components require a second-order nonlinearity - a $\chi^{(2)}$, which is normally absent in glass owing to its inversion symmetry. Thus, when self-organized frequency doubling was first discovered wide-ranging studies ensued into the mechanism and properties of this unexpected phenomenon. The mystery of photoinduced $\chi^{(2)}$ gratings was finally solved on the basis of a new physical phenomenon - the coherent photogalvanic effect, consisting in quantum interference, which excites a phase dependent current (coherent photocurrent). Coherent photocurrent induces quasi-phase matching $\chi^{(2)}$ gratings. More recently the value of nonlinearity has been increased to a level, comparable to the best nonlinear crystals by new poling techniques. Moreover in the experiments on fibre electric-field poling the first evidence of phase dependent modulation of a total cross-section of ionization due to quantum interference (coherent photoconductivity) in solid state materials has been obtained

Introduction

More than one decade has passed since the discovery of self-organized (photoinduced quasi-phase-matched) second-harmonic generation (SHG) in optical fibers [1-2]. This discovery has attracted considerable interest world-wide [3-25] due to the unusually strong $\chi^{(2)}$ (second-order susceptibility) gratings induced purely by optical fields in glass (10^{15} - 10^{16} m/V, which were 4-5 orders of magnitude higher than one could explain by known physical processes). In 1991 the value of $\chi^{(2)}$ has been increased to a new level of 1 pm/V by thermal poling [38].

The mystery of photoinduced $\chi^{(2)}$ gratings was finally solved on the basis of a new phenomenon - the coherent photogalvanic effect [6]: quantum interference between the one- and two-photon ionization processes of defect states changes the angular distribution of photoelectrons and excites a phase dependent current (*coherent photocurrent*); this current gives rise to a spatially-oscillating electrostatic field which induces the $\chi^{(2)}$ in proportion to the $\chi^{(3)}$.

More recently, the interference between different quantum processes has been the subject of considerable attention in many areas of physics (e.g. electromagnetically induced transparency (EIT) and lasers without inversion are based on quantum interference [29]). One of the reasons for this growing interest is that such kinds of interference open a prospect of a new degree of freedom in the control of physical and chemical processes - not only by the intensity or the polarization of light, but also

by the phase of light. *Coherent photocurrent* was observed in the experiments on rubidium atoms [30] and photoemission from Sb-Cs photocathodes [31] and in AlGaAs/GaAs quantum well superlattices [32]. However self-organized SHG in glass was the first observed phenomenon where *coherent photocurrent* was involved.

Until recently, two interesting aspects of the quantum interference phenomenon have not been investigated. Firstly, experiments on quantum interference have been carried out only in centrosymmetric media although it was already widely discussed that in media without inversion symmetry the interference between one- and two-photon transitions induced by light at frequencies 2ω and ω can lead to a modulation of the total cross-section for the overall transition [33]. Secondly, the modulation of the total cross-section of ionizing transitions due to quantum interference involving even number of photons (*coherent photoconductivity*) has been observed only in atomic systems [34-36]. Recently, we reported the observation of efficient SHG in glass subjected to a strong external electrostatic field [37]. The spatial periodic modulation of the applied electric field, responsible for the second harmonic signal, arises from the interaction of the intense light at frequencies ω and 2ω with glass, which has its inversion symmetry broken by the applied field. The observed phenomenon represents the first evidence of *coherent photoconductivity* in solid state materials.

On the other hand during the past seven years a number of glass poling techniques have emerged that produce permanent second-order nonlinearities

(independent of the presence of optical fields at ω and 2ω) approaching 1 pm/V (very close to the value of nonlinearity in LBO, which is a crystal widely used for pulsed frequency conversion) [38-64]. Considering that tens of cm-long interaction lengths are feasible in optical fibre (compared to a few cm in ferroelectric crystals), that the optical damage threshold is very high, and that the dispersion of refractive index is weak, nonlinearities of this order place glass in the unexpected position of serious potential competitor to the best nonlinear crystals.

In the paper, we discuss physics and potential applications of second-order nonlinearities induced by different techniques in glasses and optical glass waveguides.

The mystery of photoinduced SHG

Photoinduced SHG in glass optical fibres has been observed in two kinds of experiments. In the first kind only strong infrared (e.g. 1064 nm) pump is launched into a Ge-doped fibre and green second harmonic (SH) light exponentially grows with time and begins to saturate after many hours [1]. In this process amplification of a weak SH seeding light generated via higher-order nonlinearities, such as surface nonlinearities at the core-cladding interface and nonlinearities resulting from quadrupole and magnetic-dipole moments, is observed. We refer this kind as the self-seeded photoinduced SHG. In the second kind the infrared pump and the green SH light (seeding light) generated by an external frequency doubler are launched simultaneously into the fibre [2]. After relatively short preparation time (several minutes) the seeding light is blocked and the efficient generation of the SH light in the fibre could be observed. The high efficiencies for the SHG process (up to several %) are unexpected since the $\chi^{(2)}$, vanishes for centrosymmetric materials such as silica. It should be pointed out that the self-seeded regime has been observed only in optical fibres, however, an externally seeded regime is typical for fibres as well as for bulk glass samples. There were two crucial problems in the understanding of the phenomenon. The first one was the explanation and experimental demonstration of the high efficiency of the process by a $\chi^{(2)}$ grating which arises in glass as a result of the third-order parametric process and which automatically satisfies the condition of quasi-phase-matching between the pump and second harmonic [2-4]. The $\chi^{(2)}$ grating idea was suggested and experimentally confirmed shortly after the observation of the phenomenon. However it turned out that the most challenging problem was to find a physical mechanism which can explain the high amplitude of the $\chi^{(2)}$ grating. The electrostatic field associated with the third-order parametric mixing was too small (3-4 orders of magnitude) to explain the observed value of the $\chi^{(2)}$ nonlinearity [5]. The

mechanism of amplification of a weak seeding SH light was also a puzzle.

To explain photoinduced SHG in glasses and glass optical fibres two groups of models have been suggested, some based on macroscopic charge separation of charges (due to coherent photogalvanic effect [6] or diffusion [20]) and the other, the major part of models based on the orientation of dipoles or microscopic charge separation [2-4].

The coherent photocurrent and photogalvanic model of photoinduced frequency doubling

The mystery of the photoinduced SHG and $\chi^{(2)}$ gratings in glass and glass fibres was finally solved on the basis of a new phenomenon - the coherent photogalvanic (or photovoltaic) effect [6]. The coherent photogalvanic effect consists in the photocurrent (or the coherent photocurrent) which is excited in glass as a result of interference between one-photon ionization by light at frequency 2ω and two-photon ionization by light at frequency ω [6]. Indeed, the probability P of simultaneous ionization of defect site by two photons at frequency ω and one photon at frequency 2ω is given by:

$$P \sim |a_2 E_\omega E_\omega + a_1 E_{2\omega}|^2 = |a_2|^2 I_\omega^2 + |a_1|^2 I_{2\omega} + 2\text{Re}\{a_1^* a_2 E_\omega E_\omega E_{2\omega}^*\},$$

where E_ω and $E_{2\omega}$ are the fields amplitudes at frequency ω and 2ω respectively, I_ω and $I_{2\omega}$ are the corresponding intensities and a_1 and a_2 are two complex coefficients which determine the weight of the different processes in the probability P . The first two terms, proportional to even powers of the electric fields, describe the photoconductivity σ :

$$\sigma \sim |a_2|^2 I_\omega^2 + |a_1|^2 I_{2\omega}$$

and the last term, proportional to odd power of the fields, describes the coherent photocurrent j_{coh} or the modulation for the angular distribution of photoelectrons:

$$j_{\text{coh}} \sim 2\text{Re}\{a_1^* a_2 E_\omega E_\omega E_{2\omega}^*\}.$$

Therefore the coherent photocurrent spatially oscillates with a period Λ determined by the refractive index mismatch between light waves at frequencies ω and 2ω :

$$j_{\text{coh}} \sim \cos 2\pi z/\Lambda, \quad \Lambda = \lambda/2(n_{2\omega} - n_\omega),$$

where λ is the wavelength in vacuum of the light at frequency ω , $n_{2\omega}$ and n_ω are the refractive indices at frequencies 2ω and ω respectively. This photocurrent gives rise to an electrostatic (dc) field E_g (photogalvanic field): $E_g = j_{\text{coh}}/\sigma$. The magnitude of the photogalvanic field E_g in glass is typically $\sim 10^4$ - 10^5 V/cm and this field can induce a modulation in the $\chi^{(2)}$ via the third-order nonlinearity:

$\chi^{(2)} = 3\chi^{(3)} E_g \sim \cos 2\pi z/\Lambda$. Assuming $\chi^{(3)} = 1.8 \times 10^{-22} (\text{m/V})^2$ for silica glass, the amplitude of $\chi^{(2)}$ is $\sim 10^{16}$ - 10^{15} m/V. It turns out that the $\chi^{(2)}$ periodicity can compensate for the phase velocity mismatch

(refractive index mismatch), thus making the SH process efficient.

The coefficients a_1 and a_2 in the expression of the probability P can depend on the pump and second harmonic intensities: $a_1 = a_1(I_\omega^2, I_\omega^3, I_{2\omega})$, $a_2 = a_2(I_\omega^2, I_\omega^3, I_{2\omega})$. The physical interpretation of such dependence consists in the following: the ground level of the defect site in the one- and two-photon ionizing transitions can be populated from other defect levels, lower in energy and more densely populated. The last transition could be produced by one-photon (2ω photon or 3ω photon, generated as a result of the third harmonic generation) or two-photon ($\omega + \omega$ or $\omega + 2\omega$) absorption or absorption of even more number of photons.

It should also be noted that the higher order coherent photocurrents involving the interference of more than three coherent photons are also possible. However, each additional photon decreases the probability of the phenomenon as factor of E/E_a , where is the interatomic field strength.

It is possible to interpret the coherent photocurrent in glass in terms of electronic wave-functions interference [32]. Indeed, in centrosymmetric media one-photon transition is allowed between states of different parity and two-photon transition between states of the same parity. If the ground state for one- and two-photon transitions is the same, then the parity of the corresponding excited states should be different. The interference of electronic wave- functions of different parity in the continuum of states (conduction band) results in asymmetric wavefunction, leading to photocurrent.

The orthogonality of the wave-functions in the excited state of the one-and two-photon transitions in centrosymmetric media leads also to the absence of modulation of the total cross section of ionization (coherent photoconductivity) in this process

The coherent photogalvanic effect can take place via intro-band, inter-band and impurity-band transitions. Let us consider in more detailed way the origin of this phenomenon in Ge-doped silica glass. In this glass and where the impurity-conduction band transitions are more likely to be responsible for the phenomenon. It is well known that the defects such as Ge-Si wrong bonds (with the concentration of 10^{19} cm^{-3}) can exist in such glass [26]. These centres produce a strong absorption band at 5 eV (240 nm, singlet-singlet transition), a weak absorption band at 3.7 eV (330 nm, forbidden singlet-triplet transition) and blue triplet-singlet luminescence at 3.1 eV with a decay time of about $80 \mu\text{s}$ [27-28]. The long-lived triplet state is one of the most likely impurity levels (intermediate levels) to be responsible for the coherent photogalvanic effect. Indeed this level is located relatively close to the conduction band (within 3 eV) and the tail of conduction band can be reached from this level by the two ionizing transitions - via two infrared photons or one green photon and quantum interference between these two

path can excite coherent photocurrent. There are two possible channels of the population of this level by the photons of strong infrared pump or the photons of UV third-harmonic light generated by this pump. The first channel is the singlet-singlet transition as a result of the absorption of five or four photons of the pump or alternatively one photon of the UV and one or two photons of the pump and quick nonradiative decay (with a decay time 1 ns) to the triplet level. The second channel is the direct singlet-triplet transition as a result of the absorption of three or four photons of the pump or alternatively of the absorption of one UV photon or one UV photon and one infrared photon.

The mechanism of photoinduced amplification of the SH signal in optical fibres

Another challenging problem of the phenomenon of photoinduced SHG in optical fibres was the explanation of the mechanism of amplification of a weak SH seeding [6]. To explain this process let us consider well known equation which describes SHG

$$\partial E(2\omega) / \partial t = -i4\pi/n(2\omega)c E^2_0(\omega) \chi^{(2)} \exp(i\Delta kz) - \alpha/2 E(2\omega),$$

where α the losses.

It is necessary to add the equation for $\chi^{(2)}$. We consider that $\chi^{(2)}$ appears under the action of electrostatic field E_g induced by the coherent photocurrent. Then, from the continuity equation

$$\partial \rho / \partial t = -\text{div}(\mathbf{j} + \sigma E_g) \text{ and } \chi^{(2)} = 3\chi^{(2)} E_g,$$

it follows

$$\partial \chi^{(2)} / \partial t = 4\pi\chi^{(3)}/\epsilon \mathbf{j} - \chi^{(2)}/\tau,$$

where $\tau = \epsilon/4\pi\sigma$, ϵ is a permittivity. Neglecting non-resonance terms and converting to equations for real amplitudes and phases ($E(2\omega) = \sqrt{[8\pi/n(2\omega)c]} \sqrt{I} \exp(i\varphi)$, $\chi^{(2)} = \chi \exp[i(\Phi - \Delta kz)]$, where I is an intensity), we obtain the following set of equations

$$\begin{aligned} \partial I / \partial z &= \gamma \chi \sqrt{I} \sin(\Phi - \varphi) - \alpha I \\ \partial \varphi / \partial z &= -\gamma/2 \chi \sqrt{I} \cos(\Phi - \varphi) \\ \partial \chi / \partial t &= \delta \sqrt{I} \cos(\varphi - \Phi + \psi) - \chi/\tau \\ \partial \Phi / \partial t &= \delta/\chi \sqrt{I} \sin(\varphi - \Phi + \psi) \end{aligned}$$

where $\gamma = A \omega I_0(\omega)$, $\delta = -A(12\pi\chi^{(3)}/\epsilon)\beta I_0(\omega)$, $A^{-2} = (8\pi/c)^{-3} n^2(\omega) n(2\omega)$.

The above equations are analogous to the equations describing the dynamic self-diffraction of light beams (Kukhtarev equations) and are called Kazansky-Stepanov-Kukhtarev (KSK) equations.

It follows from these equations that the SH intensity increases with increase of fibre length under the condition $\Phi - \varphi > 0$, i.e. at the presence of the shift of the grating relative to the "interference" pattern

$(E_0^2(\omega) E(2\omega) \exp(-i\Delta kz) + cc)$ and fulfilment of the threshold condition

$$\gamma \chi^{(2)} / \sqrt{I(2\omega)} \sin(\Phi - \varphi) \geq \alpha$$

It is also evident from the KSK equations that the SH amplification in the stationary state ($\partial\chi/\partial t = 0$, $\partial\Phi/\partial t = 0$, $\Phi - \varphi = \psi$) is possible only for non-local response of the medium ($\psi \neq 0$). Let us consider in more detailed way the case of local ($\psi = 0$) response of the medium, which was experimentally observed [18-19]. Then the phase shift between the $\chi^{(2)}$ grating and the "interference" pattern (the pattern of photocurrent oscillations) is absent in the stationary state and the growth of SH intensity does not occur: $I(2\omega) \approx I_0(2\omega)$ (at $\alpha = 0$), $\chi = \delta \tau \sqrt{I_0(2\omega)}$, where $I_0(2\omega)$ is the seed radiation intensity. However, the amplification is possible in the non-stationary state ($\partial\Phi/\partial t \neq 0$). It can be expressed physically in the following way. During the writing, the grating moves along the fibre, following the movement of the "interference" pattern with some delay due to the inertia of the erasure. The SH generation in phase with the seeding SH signal occurs at the shifted component of the grating and they strengthen each other.

Observation of charge separation due to the coherent photogalvanic effect: experimental prove of the photogalvanic model of photoinduced SHG

Many experiments have been carried out to test different models of the phenomenon of photoinduced SHG and $\chi^{(2)}$ gratings. The experimental results in favour of the models based on macroscopic charge separation (via coherent photogalvanic effect or diffusion) did not contradict models explaining the phenomenon on the basis of the dipole orientation. Comparison of the experimental and calculated dependencies of the SHG efficiency on the ratio of the size of the illuminated region to the grating period allowed one to draw a definite conclusion in favour of the photogalvanic model [21]. Nevertheless, such test was connected with complicated experiment and calculation. Simple and convincing test was necessary for the final conclusion. Such test of the $\chi^{(2)}$ models in glass was made by the two very elegant experiments in which $\chi^{(2)}$ spatial distributions were probed [6, 21]. These two experiments resolved the long lasting controversy between different models in favour of the photogalvanic model (at least in single-phase oxide glasses).

Experimental test of $\chi^{(2)}$ distribution

In the first experiment the sample from Ge-doped ($\text{GeO}_2 \sim 8 \text{ mol } \%$) VAD preform was used. The sample was seeded with the SH of a mode-locked

and Q-switched Nd:YAG laser. The pump and seeding radiation were focused inside of the sample. After the preparation the seeding radiation was blocked and the induced SH signal was focused via a microscope objective onto the CCD array. The shape of the SH spot remained close to Gaussian when the sample was displaced in the direction perpendicular to the green seeding polarization. However, the shape of the SH spot changed continuously when the sample was displaced in the direction parallel to the green seeding polarization: a gap in the distribution appeared (Fig. 1).

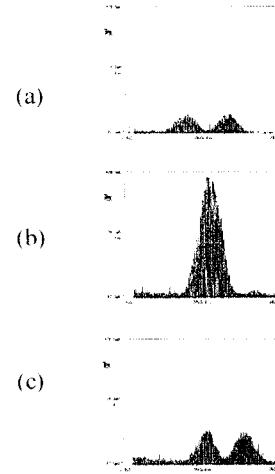


Fig.1: SH spatial distribution displayed via CCD array and oscilloscope: pump beam is shifted $\pm 13 \mu\text{m}$ (a,c) and unshifted (b) from the location of a glass region with $\chi^{(2)}$ grating.

Moreover the SH signals from the opposite sides of the gap were π out of phase. Such transformations of the shape of the SH spatial distribution were in very good agreement with the predictions of the photogalvanic model: a) the gaps in the intensity distribution correspond to the locations of space charge regions (positive and negative), where the electric field components responsible for the SH signal are close to zero and b) π out of phase SH signals are generated by the regions from the sides of the space charge, where the electric field has opposite directions. It was possible to draw two conclusions from the results of this experiment: a) diffusion can be excluded because it can produce only nondipolar charge distributions and b) such distributions are very difficult to explain if dipole alignment is responsible for the phenomenon. However some persistent followers of the dipole orientation models still argued that even dipole alignment could produce similar patterns.

**Modified experimental test of $\chi^{(2)}$ distribution:
the final defeat of dipole orientation models**

The final test of the models of photoinduced SHG was made on the basis of very simple idea [6]. Indeed, one of the basic differences between orientational and charges separation models of the phenomenon consists in the essential role of the boundary (e.g. the boundary of the illuminated region) in macroscopic charge separation. In the latter models the appearance of the electrostatic field and second-order susceptibility is impossible without the existence of boundaries which accumulates charges. In other words, the charges at the boundaries and the electrostatic field between them are the cause of the $\chi^{(2)}$. In contrast, in the orientational models the cause of the $\chi^{(2)}$ is the orientation of dipoles inside the medium (e.g. inside the illuminated region) and the existence of the boundary is not essential. Therefore the mechanism of the phenomenon can be ascertained by an experiment that can reveal the role of the boundary.

In particular, the photogalvanic model explains the origin of the $\chi^{(2)}$ by the electrostatic field resulting from the macroscopic separation of charges and their capture by empty traps at the boundaries of the illuminated region. Charges separate in the direction of light polarization when the pump and SH are polarized in the same direction. If the magnitude or sign of the space charge at one of the boundaries is altered, the electrostatic field and $\chi^{(2)}$ in the region between the charges must alter too. Such influence

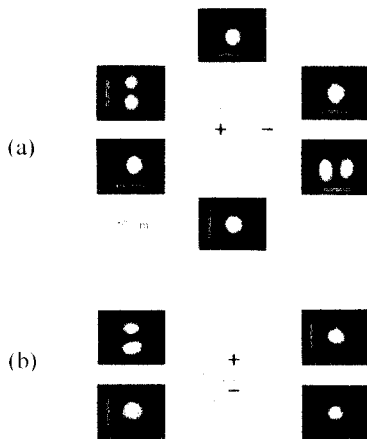


Fig.2: Distributions of the space charge and photographs of the SH near field patterns in glass samples prepared via displacement parallel (a) and perpendicular (b) to the light polarization. The directions of SH polarization are shown by arrows.

on the charge at the boundary can be realised by repeated preparation after displacement of the sample along the direction of charge separation at a distance smaller than the distance between charges (e.g. the

beam diameter). During such procedure one of the boundaries will be continuously destroyed (displaced) while the other one will be simply extended. Thereby, an extended region of charge of a certain sign separated from a small charged region of the opposite sign must appear (Fig.2). The electrostatic field along the direction of charge separation and the corresponding $\chi^{(2)}$ components must be non-zero in the three regions: at two edges of the prepared region and in the region of the final location of the writing beams. (Fig.2) The electrostatic field perpendicular to the direction of charge separation and corresponding $\chi^{(2)}$ components must be non-zero at the sides in the vicinity of the space charge regions (Fig.2). An analogous procedure of repeated sample preparation, followed by displacement in the direction perpendicular to the light polarization (direction of charge separation) will not lead to the destruction of the space charge at the boundaries. Such procedure results in the formation uniformly charged region in the direction of the sample displacement.

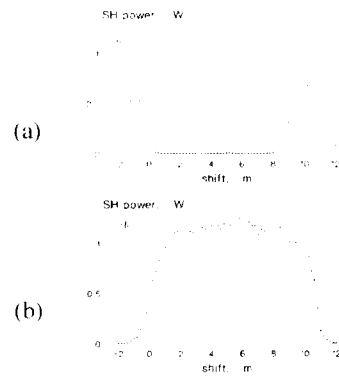


Fig.3: SH intensity distributions in glass sample prepared by displacement parallel (a) and perpendicular (b) to the direction of light polarization. Zero shift corresponds to the initial position of the sample. Note that the shift scale should be multiplied by a factor of 5.

On the other hand, in the case of dipole alignment or microscopic charge separation it is possible to prepare extended $\chi^{(2)}$ regions in any direction.

Described above experimental tests of the role of the boundary were carried out in single-phase glasses (such as lead-silicate glass and Ge-doped glass), as well as in glass doped with $\text{CdS}_x\text{Se}_{1-x}$ semiconductor microcrystallites. Experimental results obtained in single-phase glasses showed an excellent agreement with the predictions of the photogalvanic model, which was the first complete experimental evidence of the coherent photogalvanic effect (Fig3).

However the experiments carried out in semiconductor doped glasses showed different

results: it was possible to prepare extended $\chi^{(2)}$ regions in any direction (Fig.4)!

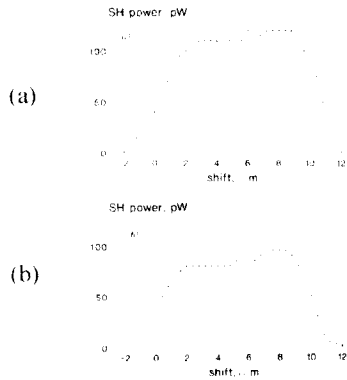


Fig.4: SH intensity distributions in semiconductor doped glass prepared via displacement parallel (a) and perpendicular (b) to the direction of light polarization. Note that the shift scale should be multiplied by a factor of 5.

One could easily explain this result by the microscopic charge separation (via the coherent photogalvanic effect) within the microcrystallites, which is expected in such glasses. The result obtained in semiconductor doped glasses gave an excellent example of the modified test of $\chi^{(2)}$ distribution in the materials without macroscopic charge separation.

The last battle: coherent photogalvanic effect (dipolar charge distribution) versus diffusion (nondipolar charge distribution)

An interesting and instructive episode in the struggle between different models of the photoinduced SHG has happened relatively recently when the experiments on direct mapping of the charge distribution inside glass were carried out [22]. The samples of borosilicate glass were etched after simultaneous irradiation of the sample by light at frequencies ω and 2ω . Two-lobe etched patterns were observed, which were interpreted as the evidence of nondipolar charge distribution in glass. This was also consistent with the *far-field* pattern of the SH generated in the sample, which also turned out to have a two-lobe shape. However these conclusions arise two questions. Firstly, does etching give adequate information about charge distribution and symmetry of electric field in glass? Secondly, is it correct to use the far-field distribution to elucidate the electric field symmetry in glass? Indeed, apart from the presence of electric field some other physical or chemical transformations in the glass during illumination with intense light, e.g. stresses, may affect the etching process. Instead, in our opinion the optical probing using SH generation, when properly used, is a better technique, which gives direct information about the symmetry of the

space charge field in glass. This technique is based on detecting the *near-field* (not far-field) SH pattern, since the SH in glass is generated where the electric field exists. It is important to point out, that the far-field pattern, which is the Fourier transform of the near-field distribution, may be significantly different from the near-field pattern. Photoinduced SH near-field distributions reported so far in different glasses, such as Ge-doped silica or lead-silicate, showed three-lobe near-field patterns, which depending on the intensity of the side lobes, produce two-lobe or one-lobe pattern in the far-field. This is in agreement with the dipolar charge distribution predicted by the coherent photogalvanic effect [23].

However, perhaps borosilicate glass SK5 behaves differently from the other glasses? To test this suggestion, we used the same type of glass as in [22] - borosilicate glass SK5 from Schott and reproduced experimental conditions very close to those reported in [22]. The 1064 nm laser beam from a mode-locked and Q-switched Nd:YAG laser was focused into a SK5 sample by using a lens with ~ 10 cm focal length. The Rayleigh distance of our IR probe (pump) beam ($z_R = \pi\omega^2 n/\lambda$) was ~ 3.5 mm. We used two samples in our experiments: one was 1 cm long and the other one was 1 mm long, thus the confocal parameter ($L/2z_R$) for the first and second samples is 1.4 and 0.14 respectively. We used thin samples in order to test the validity of our near-field measurements (to ensure that the SH pattern, we are imaging, is generated in the focal plane of the probe beam). We prepared the samples with the encoding peak intensities of ~ 4 GW/cm² and ~ 1 GW/cm² for the fundamental and SH beams respectively. Photoinduced SH far-field patterns from the thick and thin samples show a two-lobe structure (Fig.5), which looks very similar to that reported in [22].

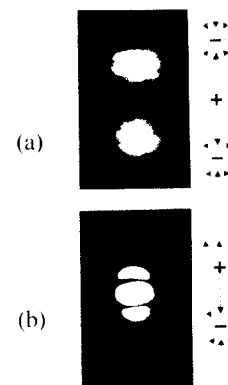


Fig.5: Photograph of the two-lobe SH far-field pattern generated in SK5 glass in our experiments with corresponding interpretation of the pattern on the basis of the nondipolar charge distribution [22](a). The three-lobe SH near pattern and the corresponding real charge distributions in SK5 glass (b). This three-lobe pattern in the near field is observed as two-lobe pattern in the far field.

However, the near-field pattern is quite different from the far-field pattern and shows a well defined three-lobe structure (Fig. 5). These three-lobe patterns are in excellent agreement with the dipolar charge distribution (Fig.5), as a result of the directional charge separation by the coherent photocurrent and is in contradiction with the nondipolar charge distribution in this glass revealed by using etching techniques [22].

Electrically stimulated light-induced frequency doubling: evidence of coherent photoconductivity

Fibres with the internal capillaries suitable for inserting internal electrodes are very attractive to use in the poling experiments [9, 10, 42].

During the experiments on fibres with internal electrodes we observed a new physical phenomenon, which was named the electrically stimulated light-, induced growth of $\chi^{(2)}$ gratings [37]. Firstly, only infrared light of ~ 12 mW average power (1 kW peak power) for ~ 1 hour was launched into the fibre, ~ 25 cm long. A mode-locked and Q-switched Nd-YAG laser operating at 1064 nm was used as the pump source. No SH generation was observed in the fibre. Then the pump of ~ 12 mW average power and the SH seeding of ~ 40 μ W average power were launched simultaneously. The SH seeding was removed after preparation of ~ 10 min and a SH signal of ~ 20 μ W average power was observed, corresponding to a conversion efficiency of $\sim 0.16\%$. This was confirmed by monitoring the growth of the SH signal in the fibre when the SH seeding was blocked for a short time during the preparation (Fig. 6). This result is in good agreement with previous observations on photoinduced SHG in Ge-doped fibres [1-2] and may be explained by the appearance of a $\chi^{(2)}$ grating in the fibre.

High voltages up to 10 kV (corresponding to electrical fields $\sim 10^7$ V/cm) across the electrodes inside the fibre were then applied and infrared pump of ~ 1 kW peak power was launched into the fibre. For applied voltages greater than ~ 2 kV a strong increase of a weak electric-field induced second harmonic (EFISH) signal of ~ 10 nW (i.e. generated immediately after the electric field was applied) was observed (Fig. 6).

During these experiments we achieved conversion efficiencies as high as $\sim 2\%$ for a peak pump power of ~ 1 kW, which is ~ 10 times higher than in the experiments carried out without applying an external electric field.

The high conversion efficiency measured and the observed quadratic dependence of the SHG efficiency on the fibre length represent clear evidences of quasi-phase-matched SHG due to presence of a $\chi^{(2)}$ grating in the fibre.

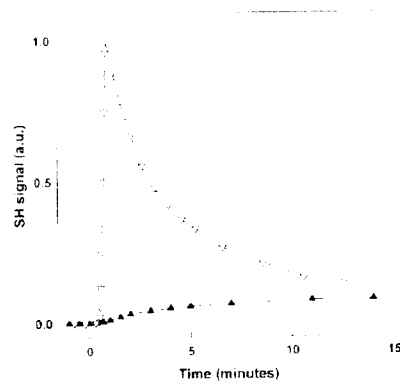


Fig.6: Time dependence of SH signal in a fibre with external SH seeding of ~ 40 μ W average power (filled triangles). The seeding was launched at $t = 0$. Time dependence of SH signal in a fibre with applied voltage of 5 kV (opened triangles). The voltage was switched on at $t = 0$.

These experimental results can be explained as follows. Let us consider interaction of light beams of frequencies ω and 2ω in glass when a strong dc electric field ($E_0 \gg E_g$) is applied. The probability of simultaneous ionization of defect site by two photons at frequency ω and one photon at frequency 2ω in the presence of E_0 is given by:

$$P \sim |a_2 E_\omega E_\omega + b_2 E_0 E_{2\omega}|^2 = |a_2|^2 I_\omega^2 + |b_2|^2 I_{2\omega} E_0^2 + 2\text{Re}\{a_2 b_2^* E_0 E_\omega E_\omega E_{2\omega}^*\}.$$

All terms in this expression are even powers of the electric field regardless they are uniform (first two terms) or modulated (being dependent on the relative phase of the fields at frequencies ω and 2ω (the last term)). Unlike in the process without dc electric field considered above, the modulated part of the probability leads to modulation of the total ionization cross section and hence to a corresponding modulation of the photoconductivity:

$$\sigma = \sigma_0 + \sigma_{\text{coh}},$$

where

$$\sigma_0 \sim |a_2|^2 I_\omega^2 + |b_2|^2 I_{2\omega} E_0^2$$

is the uniform part of the photoconductivity and

$$\sigma_{\text{coh}} \sim 2\text{Re}\{a_2 b_2^* E_0 E_\omega E_\omega E_{2\omega}^*\} \sim \cos 2\pi z/\Lambda$$

is the part of the photoconductivity being dependent on the relative phase between E_ω and $E_{2\omega}$ (coherent photoconductivity).

The ohmic current ($j = \sigma E_0$) induced by the applied electric field separates photocarriers which accumulate at the boundaries of the illuminated region and screen the applied electric field E_0 . The resulting internal electric field inside the glass E_c evolves accordingly to:

$$dE_c/dt = -E_c/\tau, \tau = \epsilon/\sigma,$$

where τ is the dielectric relaxation time and ϵ is dielectric constant of glass. An approximate solution for E_c in the limit $\sigma_{\text{coh}} \ll \sigma_0$, $\tau = \tau_0 = \epsilon/\sigma_0$ is:

$$E_c = \sigma_{\text{coh}}/\sigma_0 E_0 \{1 - \exp(-t/\tau_0)\} \exp(-t/\tau_0) + E_0 \exp(-t/\tau_0) = E_c^{\text{coh}} + E_c^0,$$

where E_c^{coh} and E_c^0 are the modulated and uniform part of the internal electric field. The modulated part of the electric field, proportional to σ_{coh} , and the corresponding $\chi^{(2)} = 3\chi^{(2)} E_c^{\text{coh}}$ are zero at the beginning ($t=0$), reach maximum values at $t = \tau_0 \ln 2$ and finally decreases to zero in the steady state condition ($t=\infty$).

It should be noted that no modulation of the angular distribution of photoelectrons takes place in a process, such as the above interference, where one- and two-photon ionizing transitions in a strong dc electric field ($E_0 \gg E_p$) are involved.

Our experimental results can be qualitatively interpreted in the light of the mechanism presented above, i. e. on the basis of photoconductivity being dependent on the relative phase between interacting waves at frequencies ω and 2ω , which provides quasi-phase-matching for the SH generation. From the measurements we can also estimate the amplitude of the second-order susceptibility $\chi^{(2)} = 10^{-14}$ m/V, which corresponds to a modulation of $\sim 8\%$ in the applied electric field.

New poling techniques: towards practical second-order nonlinearity in glass

During the past decade a number of glass poling techniques have emerged that produce permanent $\chi^{(2)}$ approaching 1 pm/V. These new poling techniques are: thermal poling at 250-300°C under an applied high voltage (the second-order nonlinearity appears in a thin layer just under the anode) [38], corona poling of glass waveguides [39] and charge implantation by exposure to an electron-[40] or proton-beam [41]. Most recently an electro-optic coefficient of ~ 6 pm/V has been reported in silica fibre poled under UV excitation [42]. However other groups have not confirmed the latter result. So far thermal poling is the most promising technique for practical applications: nonlinearity is strong enough and shows no degradation under illumination with intense visible and infrared light [43-64]. It was suggested that a high dc field ($\sim 10^7$ V/cm) in a thin region (~ 5 - 10 μm) depleted of cations under the anodic surface is responsible for this phenomenon [37]. This field can be frozen-in between the two layers of space charge: negatively charged depletion region and positively charged layer created as a result of ionization or diffusion in the high field between the depletion region and the anode [50]. Charged distributions obtained in poled glasses by the laser induced pressure pulse (LIPP) [54] and the etching technique [55] are in good agreement with this model. More complicated charge distributions (with the inverted charge regions) were also observed by the LIPP technique in poled samples [54]. It is still not clear whether $\chi^{(2)}$ is induced by high dc field via

$\chi^{(3)}$ or orientation of dipoles. Indeed with the maximum dc field limited by the intrinsic breakdown of silica ($\sim 10^7$ V/cm) it is possible to justify the values of $\chi^{(2)} \leq 5$ pm/V via $\chi^{(3)}$ of silica. However about two times higher values have been measured experimentally. This discrepancy may have different explanations: by uncertainty in the thickness and distribution of the nonlinear layer, by a higher $\chi^{(3)}$ value in the poled layer, or by orientation of dipole defects (taking into account the number of defects available in silica glass for the latter to be true the hyperpolarizability of each defect must be unrealistically high).

A problem encountered in thermal poling is the spreading out of the poled regions caused by air breakdown that occurs when one attempts to create QPM $\chi^{(2)}$ gratings [45, 46]. Two solutions are possible to side-step this problem: 1) electron beam or UV light can be used for selective erasure of uniformly poled sample [43]; 2) thermal poling in vacuo, using a patterned electrode, can create periodic $\chi^{(2)}$ patterns [51]. Continuous wave QPM frequency conversion to the blue has also been demonstrated in D-shaped optical fibres using patterned anodic electrode on the plane side, followed by thermal poling in vacuo. In the first work on frequency conversion to the blue at 430 nm [51], the maximum blue light power (in the $\text{LP}_{11}^{2\omega}$ second-harmonic (SH) mode) detected was ~ 400 pW, corresponding to a fundamental power in the fibre of ~ 100 mW. In a more recent work [59] blue light has been generated in the fundamental mode $\text{LP}_{01}^{2\omega}$, with an increase of a factor of ten in the conversion efficiency in comparison with the previous results. The interaction with the higher order SH modes were suppressed by side etching of the fibre surface. Uniformly poled fibres were also tested by using a tuneable cw Ti:sapphire laser. Maker's oscillations of SH signal were observed corresponding to the value for the $\chi^{(2)}$ in the uniformly poled fibre of ~ 1.4 pm/V. When periodic poling was produced in the fibres the effective nonlinear coefficient d_{eff} was ~ 50 times smaller than the expected value of 0.22 pm/V ($=d/\pi$, $d=\chi^{(2)}/2$) for a periodic grating with an amplitude d of 0.7 pm/V, corresponding to the nonlinearity measured in the uniformly poled fibre. This degradation was mainly due to the non-uniformity of the grating (which was experimentally confirmed by direct optical image of the $\chi^{(2)}$ grating) although it is not excluded that the non-optimised overlap integral between interacting modes and poled region can still play a role in reducing the efficiency.

As we pointed out [60], compared with polar crystals waveguides, such as lithium niobate (LN) and potassium titanyl phosphate (KTP), poled silica fibres offer greater bandwidths availability (more than one order of magnitude for the same device length) because of their lower dispersion. Therefore the relatively low value of the nonlinear coefficient could be compensated by increasing the length of the

device, thus achieving the same efficiency as for the crystals without altering the frequency stability.

In the case of pulsed applications the group velocity mismatch (GVM) between pulses at different frequency determines the device length which should be the result of a good trade-off between high conversion efficiency and low pulse spreading. The low GVM in silica fibres (more than one order of magnitude less than in LN and KTP), combined with the high optical damage threshold, makes poled silica a suitable material for pulsed frequency conversion since the relatively low nonlinear coefficient (d_{eff}) can be compensated by extended interaction lengths (l_{eff}) and high peak intensities (I_p), so that the figure of merit $d_{\text{eff}}^2 l_{\text{eff}}^2 I_p$ for the conversion efficiency is maintained high.

Conclusion

During the last decade the research on photosensitivity and poling in glasses and optical glass waveguides has led to the discoveries of new physical phenomena: photoinduced SHG, electrically stimulated light-induced frequency doubling, coherent photogalvanic effect and coherent photoconductivity. Fascinating physics of quantum interference behind the discovered phenomena attracts considerable interest in many areas of modern science.

The second-order optical nonlinearities achieved by new poling technique are high enough for some applications such as frequency conversion of high power fibre lasers, generation of correlated photon pairs by parametric down-conversion for all-fibre quantum cryptography and construction of all-fibre electric-field sensors for power industry. However higher nonlinearities as high as 10 pm/V are necessary for the wide-spreading applications, especially in optical communications.

A better understanding of the mechanisms of glass poling, which are still not fully understood, may help to improve the value of second-order nonlinearity in poled glasses, perhaps to values competitive with the best ferroelectric crystals.

References

1. U. Österberg and W. Margulis, "Dye laser pumped by Nd:YAG laser pulses frequency doubled in glass optical fibre," *Opt. Lett.* **11**, 516 (1986).
2. R.H. Stolen and H.W.K. Tom, "Self-organised harmonic generation in optical fibres," *Opt. Lett.* **12**, 585 (1987).
3. N.B. Baranova and B.Ya. Zeldovich, "Extension of holography to multiwavelength fields," *JETP Lett.* **45**, 716 (1987).
4. M.C. Farries, P.St.J. Russell, M.E. Fermann and D.N. Payne, "Second harmonic generation in an optical fibre by self-written $\chi^{(2)}$ grating," *Electron. Lett.* **23**, 322 (1987).
5. V. Mizrahi, U. Osterberg, C. Krautchik, G.E. Stegeman, J.E. Sipe and T.P. Morse, "Direct test of a model of efficient second-harmonic generation in optical fibres," *Appl. Phys. Lett.* **53**, 557 (1988).
6. E.M. Dianov, P.G. Kazansky and D.Yu. Stepanov, "Problem of the photoinduced second harmonic generation," *Sov. J. Quantum. Electron.* **19**, 575 (1989); "Photovoltaic model of photoinduced second harmonic generation in optical fibres," *Sov. Lightwave Commun.* **1**, 247 (1991); E.M. Dianov, P.G. Kazansky, D.S. Starodubov and D. Yu. Stepanov, "Photoinduced second harmonic generation: observation of charge separation due to the photovoltaic effect," *Sov. Lightwave Commun.* **3**, 83 (1992).
7. F. Ouellette, K. Hill and D.C. Johnson, "Enhancement of second-harmonic generation in optical fibres by hydrogen and heat treatment," *Appl. Phys. Lett.* **54**, 1086 (1989).
8. R. Kashyap, "Phase-matched periodic electric-field-induced second-harmonic generation in optical fibres," *J. Opt. Soc. Am.* **B 6**, 313 (1989).
9. M.-V. Bergot, M.C. Farries, M.E. Fermann, L. Li, L.J. Poyntz-Wright, P.St.J. Russell and A. Smithson, "Generation of permanent optically-induced 2nd order nonlinearities in optical fibres by poling," *Opt. Lett.* **13**, 592 (1988).
10. L. Li and D.N. Payne, "Permanently-induced linear electro-optic effect in silica optical fibres," in *Digest of Conference on Integrated and Guided Wave Optics* (Optical Society of America, Washington, D.C., 1989), paper TuAA2-1.
11. V. Mizrahi, Y. Hibino and G. Stegeman, "Polarization study of photoinduced second-harmonic generation in glass optical fibres," *Opt. Commun.* **78**, 283 (1990).
12. A. Kamal, D.A. Weinberger and W.H. Weber, "Spatially resolved Raman study of self-organized $\chi^{(2)}$ gratings in optical fibres," *Opt. Lett.* **15**, 613 (1990).
13. M.D. Selker and N.M. Lawandy, "Observation of seeded second-harmonic generation in bulk germanosilicate fibre," *Opt. Commun.* **77**, 339 (1991).
14. D. Anderson, V. Mizrahi and J.E. Sipe, "Model for second-harmonic generation in glass optical fibres based on asymmetric photoelectron emission from defect sites," *Opt. Lett.* **16**, 796 (1991).
15. F. Charra, F. Devaux, J.M. Nunzi and P. Raimond, "Picosecond light-induced

- noncentrosymmetry in dye solution," *Phys. Rev. Lett.* **68**, 2440 (1992).
16. V. Dominic and J. Feinberg, "Growth rate of second-harmonic generation in glass," *Opt. Lett.* **17**, 1761 (1992).
 17. D.M. Krol, D.J. DiGiovanni, W. Pleibel and R.H. Stolen, "Observation of resonant enhancement of photoinduced second-harmonic generation in Tm-doped aluminosilicate glass fibres," *Opt. Lett.* **18**, 1220 (1993).
 18. E. M. Dianov, P.G. Kazansky, D.S. Starodubov and D.Yu. Stepanov, "Observation of phase mismatching during the preparation of second-order susceptibility gratings in glass optical fibre", *Sov. Lightwave Comm.* **1**, 385 (1991).
 19. K.W. Koch and G.T. Moore, "Two-colour interferometry using a detuned frequency-doubling crystal", *Opt. Lett.* **16** (1991).
 20. N.M. Lawandy, "Intensity dependence of optically encoded SHG in germanosilicate glass: evidence for a light-induced delocalization transition", *Phys. Rev. Lett.* **65**, 1745 (1990).
 21. E.M. Dianov, P.G. Kazansky, C. Krautschik and D.Yu. Stepanov, "Test of photovoltaic model of photoinduced SHG in optical fibres," *Sov Lightwave Commun.* **1**, 381 (1991).
 22. J. H. Kyung and N. M. Lawandy, "Direct measurement of photoinduced charge distribution responsible for SHG in glass", *Opt. Lett.* **21**, 186 (1996); "Direct observation of the effective $\chi^{(2)}$ grating in bulk glass encoded for SHG", *Opt. Lett.* **21**, 632 (1996).
 23. E.M. Dianov, P.G. Kazansky, D.S. Starodubov and D.Yu. Stepanov, "Photoinduced SHG: observation of motion of space charge regions", *Sov. Lightwave Commun.* **2**, 269 (1992).
 24. V. O. Sokolov and V. B. Sulimov, "On the phenomenological theory of the coherent photogalvanic effect in glass," *Phys. Stat. Sol. (b)* **187**, 177 (1995).
 25. W. Margulis, F. Laurell, B. Lesche, "Imaging the nonlinear grating in frequency-doubling fibres," *Nature* **378**, 649 (1995).
 26. E.J. Friebel and D.L. Griscom, "Colour centres in glass waveguides", in *Defects in Glasses*, eds. By Galeener, G.L. Griscom and M.L. Weber (Material Research Society, Pittsburgh, PA) **61**, 125 (1993).
 27. H. Hosono, Y. Abe, D.L. Kinser, R.A. Weeks, K. Muta and H. Kawazoe, *Phys. Rev.* **B46**, 11445 (1992).
 28. M. Kohketsu, K. Awazu, K. Kawazoe and M. Yamane, *Jpn. J. Appl. Phys.* **28**, 622 (1989).
 29. S. Harris, "Electromagnetically induced transparency", *Physics Today* **50**, 36 (1997)
 30. Y.Y. Yin, C. Chen, D.S. Elliot, and A.V. Smith, "Asymmetric photoelectron angular distribution from interfering photoionization processes," *Phys. Rev. Lett.* **64**, 2353 (1992).
 31. N.B. Baranova, A.N. Chudinov, A.A. Shulginov, and B.Ya. Zel'dovich, "Polarization dependence of the phase of interference between single- and two-photon ionization," *Opt. Lett.* **16**, 1346 (1991).
 32. E. Dupont, P. B. Corkum, H. C. Liu, M. Buchanan, and Z. R. Wasilewski, "Phase-controlled currents in semiconductors," *Phys. Rev. Lett.* **74**, 3596 (1995).
 33. R. J. Glauber, "Coherence and quantum detection," in *Quantum Optics* edited by R. J. Glauber, Proceedings of the E. Fermi International School in Physics, Vol. 62 (New York - London: Acad. Press, 1969).
 34. J. C. Miller, R. N. Compton, M. G. Payne, and W. R. Garrett, "Resonantly enhanced multiphoton ionization and third harmonic generation in xenon gas," *Phys. Rev. Lett.* **45**, 114 (1980).
 35. S. M. Park, S. P. Lu, and R. J. Gordon, "Coherent laser control of the resonance-enhanced multiphoton ionization of HCl," *J. Chem. Phys.* **94**, 8622 (1991).
 36. C. Chen, Y. Y. Yin, and D. S. Elliot, "Interference between optical transitions," *Phys. Rev. Lett.* **64**, 507 (1990).
 37. P.G. Kazansky and V. Pruneri, "Electrically stimulated light-induced second-harmonic generation in glass: evidence of coherent photoconductivity," *Phys. Rev. Lett.* **78**, 2956 (1997).
 38. R.A. Myers, N. Mukherjee and S.R.J. Brueck, "Large second-order nonlinearities in poled fused silica," *Opt. Lett.* **16**, 1732 (1991)
 39. .A. Okada, K. Ishii, K. Mito and K. Sasaki, "Second-harmonic generation in novel corona poled glass waveguides," *Appl. Phys. Lett.* **60**, 2853 (1992).
 40. P.G. Kazansky, A. Kamal and P.St.J. Russell, "High second-order nonlinearities induced in lead silicate glass by electron-beam irradiation," *Opt. Lett.* **18**, 693 (1993).
 41. L. J. Henry, B. V. McGrath, T. G. Alley and J. J. Kester, "Optical nonlinearity in fused silica by proton implantation," *J. Opt. Soc. Am.* **B 13**, 827 (1996).
 42. T. Fujiwara, D. Wong, Y. Zhao, S. Fleming, S. Poole and M. Sceats, "Electro-optic modulation in germanosilicate fibre with UV-excited poling," *Electron. Lett.* **31**, 573 (1995).
 43. P.G. Kazansky, A. Kamal and P.St.J. Russell, "Erasure of thermally poled second-order nonlinearity in fused silica by electron implantation," *Opt. Lett.* **18**, 1141 (1993).

44. P.G. Kazansky, L. Dong and P.St.J. Russell, "High second-order nonlinearities in poled silicate fibres," *Opt.Lett.* **19**, 701 (1994).
45. P.G. Kazansky, L. Dong and P.St.J. Russell, "Vacuum poling: an improved technique for effective thermal poling of silica glass and germanosilicate optical fibres," *Electron. Lett.* **30**, 1345 (1994).
46. R. Kashyap, G.J. Veldhuis, D.C. Rogers and P.F. McKee, "Phase-matched second-harmonic generation by periodic poling of fused silica," *Appl. Phys. Lett.* **64**, 1332 (1994).
47. A. C. Liu, M. J. F. Digonnet and G. S. Kino, "Electro-optic phase modulation in a silica channel waveguide," *Opt. Lett.* **19**, 466 (1994).
48. X.-C. Long, R. A. Myers and S. R. J. Brueck, "Measurements of the electrooptic coefficient in poled amorphous silica," *Opt. Lett.* **19**, 1819 (1994).
49. N. Mukherjee, R. A. Myers and S. R. J. Brueck, "Dynamics of SHG in fused silica," *J. Opt. Soc. Am.* **B 11**, 665 (1994).
50. P. G. Kazansky and P. St. J. Russell, "Thermally poled glass: frozen-in electric field or oriented dipoles?," *Opt. Comm.* **78**, 611 (1994).
51. P. G. Kazansky, V. Pruneri and P. St. J. Russell, "Blue-light generation by quasi-phase-matched frequency doubling in thermally poled optical fibres," *Opt. Lett.*, **20**, 843, (1995).
52. H. Nasu, H. Okamoto, K. Kurachi, J. Matsuoka, K. Kamiya, A. Mito and H. Hosono, "SHG from electrically poled SiO₂ glasses: effects of OH concentration, defects and poling conditions," *J. Opt. Soc. Am.* **B 12**, 644 (1995).
53. H. Nasu, K. Kurachi, A. Mito, H. Okamoto, J. Matsuoka and K. Kamiya, "SHG from an electrically polarized TiO₂ containing silica glasses," *J. Non-Cryst. Solids* **181**, 83 (1995).
54. P.G. Kazansky, A. R. Smith, P. St. J. Russell, G. M. Yang and G. M. Sessler, "Thermally poled glass: Laser induced pressure pulse probe of charge distribution," *Appl. Phys. Lett.* **68**, 269 (1996).
55. W. Margulis and F. Laurell, *Opt. Lett.* **21**, 1786 (1996)
56. H. Takebe, P. G. Kazansky, P. St. J. Russell and K. Morinaga, "Effect of poling conditions on SHG in fused silica," *Opt. Lett.* **21**, 468 (1996).
57. X.-C. Long, R. A. Myers and S. R. J. Brueck, "A poled electrooptic fiber," *IEEE Photon. Tech. Lett.* **8**, 227 (1996)
58. X.-C. Long and S. R. J. Brueck, "Large -signal phase retardation with a poled electrooptic fibre," *IEEE Photon. Tech. Lett.* **9**, 767 (1997).
59. V. Pruneri and P.G. Kazansky, "Electric-field thermally poled optical fibres for quasi-phase-matched second harmonic generation," *IEEE Photon. Tech. Lett.* **6**, N2 (1997).
60. P. G. Kazansky, P. St. J. Russell and H. Takebe, "Glass fibre poling and applications," *J. Lightwave Tech.* **15**, no.8 (1997).
61. V. Pruneri and P. G. Kazansky, "Frequency doubling of of picosecond pulses in periodically poled D-shaped silica fibre," *Electron. Lett.* **33**, 318 (1997).
62. P. G. Kazansky and V. Pruneri, "Electric field poling of quasi-phase-matched optical fibres," *J. Opt. Soc. Am.* **B 14**, no.11 (1997).
63. V. Pruneri, G. Bonfrate, P.G. Kazansky, C. Simonneau, P. Vidakovic and J.A. Levenson, "Efficient frequency doubling of 1.5 μ m femtosecond laser pulses in quasi-phase-matched optical fibres," *Appl. Phys. Lett.* **72**, 1007 (1998).
64. O. Sugihara, M. Nakanishi, H. Fujimura, C. Egami and N. Okamoto, "Thermally poled silicate thin films with large SHG," *J. Opt. Soc. Am.* **B15**, (1998).